Decadal wave variability in the eastern North Atlantic associated with the North Atlantic Oscillation

H. Santo[*,1], P. H. Taylor[1] and R. Gibson[2]

[1]Department of Engineering Science, University of Oxford, Oxford, UK
[2]Offshore Consulting Group, London, UK

September 19, 2015

1 Abstract

We investigate variability in time for wave records obtained from the Norwegian 10 km Reanalysis Archive (NORA10) hindcast model for the period of $1958 - 2011$. Both the mean wave field year by year (significant wave height, wave period and wave power/unit length, each averaged over a year) and extreme waves (using a storm-based criterion) are investigated at locations in the eastern North Atlantic and the northern North Sea. We seek simple linear correlations between the wave fields at each location and the North Atlantic Oscillation (NAO) and other atmospheric modes.

Preliminary results suggest the winter value of the NAO index is not a strong predictor for variability for extreme waves in the open North Atlantic west of Ireland. The correlation however improves markedly moving to north west of Shetland and offshore Norway, where the results are consistent with previous work using an older generation of hindcast model (Taylor et al. 2009, 11th International Workshop on Wave Hindcasting and Forecasting). This is in contrast to mean wave fields (and wave power) where the correlation works well for all the open North Atlantic locations. The correlation of the omnidirectional wave fields with the NAO works less well in the northern North Sea, but when the total signal is partitioned based on the incoming wave direction, a pair of anti-phase signals associated with positive or negative phases of the NAO and other modes are revealed.

We suggest that the NAO is the dominant factor behind decadal variability for the mean wave field in the eastern North Atlantic and the North Sea. For extreme waves the relationship to the NAO is somewhat weaker but still significant.

2 Introduction

This paper summarises recent findings on the decadal variability of both mean and extreme wave climates for locations in the eastern North Atlantic and North Sea, as reported in Santo et al. (2015c,b,a). We find good correlation between the wave climate variability and the dominant large scale north-south pressure anomalies (or teleconnections), which are the North Atlantic

---

[*]Corresponding author: harrif.santo@eng.ox.ac.uk

Oscillations (NAO), followed by other two atmospheric modes: the Eastern Atlantic (EA) and the Scandinavian (SCA) pattern. Similar observations have been reported for the correlation between the wave climate and the NAO alone in the eastern North Atlantic, see for example Bromirski and Cayan (2015); Reguero et al. (2015); Neill et al. (2014); Neill and Hashemi (2013); Mackay et al. (2010); Izaguirre et al. (2010); Wang and Swail (2001); Menéndez et al. (2008).

3   Data and methods

We examine 54 years worth of hindcast wave data at eight locations spread out in the eastern North Atlantic and North Sea from $1958 - 2011$, as shown in Figure 1. The hindcast data is from the Norwegian 10 km Reanalysis Archive (NORA10), for more information see Reistad et al. (2011). We also have measured buoy data for Haltenbanken and Forties. The wave data available in 3 h intervals contain information such as date, time, significant wave height (H_s), peak spectral wave period (T_p), mean wave period (T_m or T_{m01}, only in hindcast data), zero-crossing period (T_z or T_{m02}, only in measured data), wind speed, wind and wave directions.
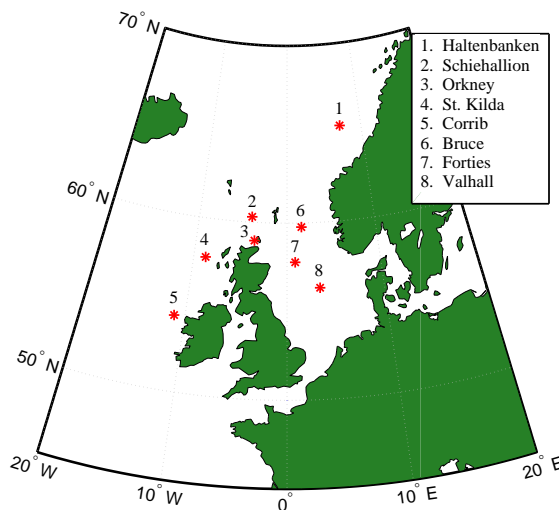

Figure 1: Map of the locations, with points 1-5 are in the eastern North Atlantic, 6-8 in the North Sea.

Model/buoy comparisons have been performed both in terms of mean and extreme value for locations in Haltenbanken and Forties, see Santo et al. (2015c,b). In general, the agreement is reasonable, with being close to 1:1 line and with normalised root mean squared error (NRMSE) of $\sim 20\%$ for H_s and T_p comparisons.

The NAO has long been known to affect climate variability in the northern hemisphere, particularly in the winter months, see for example Hurrell et al. (2003). It describes changes in the Atlantic eddy-driven jet which regulates the near surface westerly winds (Woollings et al., 2010), hence a relationship between pressure anomalies and wave climate is likely. The pattern of each atmospheric mode has been characterised as climate indices, which are obtainable from National Oceanic and Atmospheric Administration (NOAA) Climate Prediction Center (www.cpc.ncep.noaa.gov) and available from January 1950 to the present. The climate indices are derived from the rotated Empirical Orthogonal Function (EOF) analysis by Barnston and Livezey (1987).

We correlate the variability of wave climate with the winter average of the teleconnection indices (i.e. from mid October to mid April). We use a predictor model $P_{predictor}$ which consists of a linear combination of the climate indices (linear regression), expressed as:

$$P_{predictor} \quad = \quad \overline{P} \times [1 + b(EA(t) - \overline{EA}) + c(NAO(t) - \overline{NAO}) + d(SCA(t) - \overline{SCA})]$$

where $\overline{P}$ is the average wave climate over the period of available data. For mean wave climate correlation which is based on annual mean value, we impose a high-pass filter to both the EA and the SCA indices, and a low-pass filter to the NAO index, since the long timescale variation of both the EA and SCA are correlated to the NAO. For extreme wave climate correlation which is based on a sliding window, we impose a low-pass filter of 5 years to all the indices. b, c and d are non-dimensionalised constants reflecting the relative importance of the EA, the SCA and the NAO signals in predicting wave climate, respectively. The individual cut-off values of the high-pass filters and the values of the non-dimensionalised constants are chosen to minimise the variance between the wave climate signal and the predictor model in each case.

Having trained the predictor model and obtained good correlation, we can perform a reconstruction of historic wave climate at each location. To do this, we introduce proxy indices using the historical reconstructed monthly 500 mbar pressure maps computed by Luterbacher et al. (2002) from $1659 - 1998$. To produce the proxy indices, we first regress the climate indices with the pressure maps over the overlapping period from $1950 - 1998$, and average the pressure-time histories over the regions of high correlation from $1665 - 1998$ to produce the proxy indices. Reasonable agreement between the proxy and climate indices is achieved with $R^2 > 0.7$. For more details on the proxy indices and the reconstruction, see Santo et al. (2015c).

4 Mean wave power variability

We calculate the wave power per unit length of wavefront for each sea-state (termed ocean wave power resource) using:

$$P = \frac{\rho g^2}{64\pi} H_s^2 T_p$$

where ρ is the water density and g is the gravitational acceleration. Since T_p is the only available period from both the hindcast and measured data, we choose to use T_p (instead of T_e or T_m) so that model/buoy comparison can also be performed in terms of wave power. Note that T_e is not available in either type of data. We choose to look at annual mean wave power variability, with the average wave power per metre of wavefront for a year expressed in kW/m. The definition of a year is from the middle of July one year to the middle of July the subsequent year, with the year date taken from the part of the record up to December.

Figure 2(a) show the variability of mean wave power (solid lines) at Haltenbanken, Schiehallion and Forties. It can be seen that for locations in the open North Atlantic such as Haltenbanken and Schiehallion, the temporal structure is very similar. Large inter-annual and decadal variability is observed, with coefficient of variation (CV) $\sim 20\%$, defined as the ratio of the standard deviation to the mean. For locations in the North Sea such as Forties, the variability is smaller (CV = 14%) and the temporal structure is different as there is sheltering by the land surrounding the North Sea. Also on the same figure, the results of the correlation are presented (dashed lines) with the R^2 values for each location. Strong correlations are obtained between the ocean wave power resource and the predictor model for both Haltenbanken and Schiehallion ($R^2 > 0.7$), but weaker correlation for Forties ($R^2 = 0.41$).
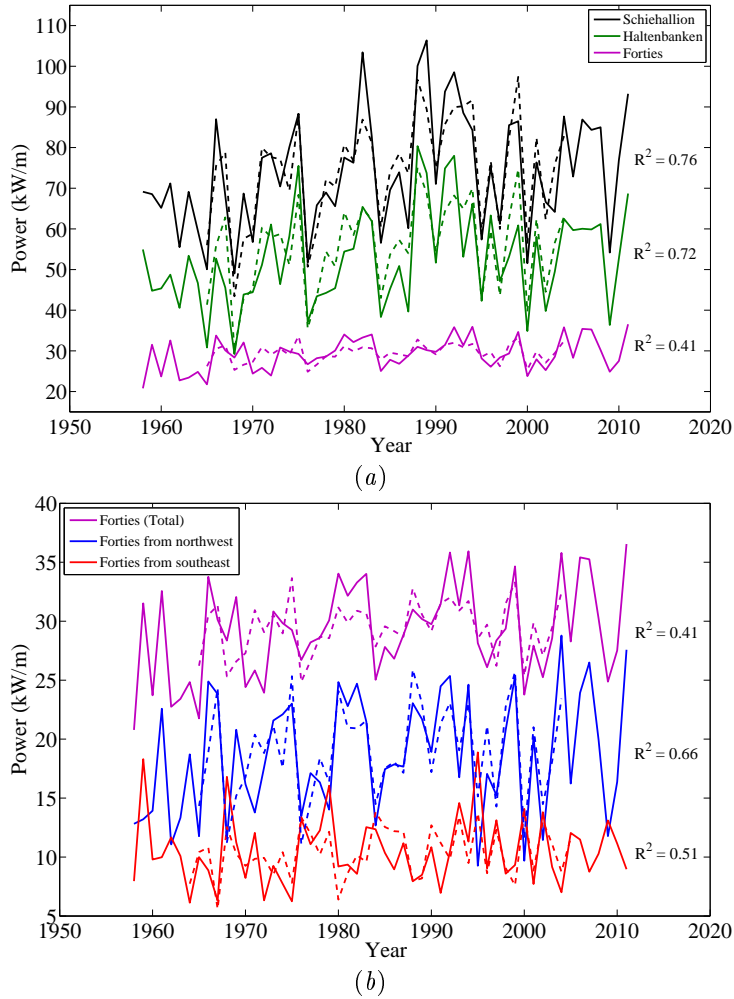
3

Figure 2: Comparison of the actual (solid lines) and predicted (dashed lines) wave power. (a) For the three locations. (b) For Forties with angle partitioning.

As demonstrated in Santo et al. (2015c), there are effectively two directionally-opposite sectors of dominant waves leading to reduced variability in the ocean wave power resource in the North Sea, as opposed to a single dominant directional sector in the open North Atlantic. Figure 2(b) illustrates the partitioning of the omnidirectional wave power at Forties into the two dominant directions: northwest and southeast. Both directional sectors are in anti-phase with each other, and they are more variable (CV = 28% for both) than the omnidirectional signal. Better correlation for each sector with the predictor model ($R^2 = 0.5 - 0.6$) demonstrates that both sectors are associated with the positive or negative phases of the NAO and other modes. The northwesterly waves in the North Sea are more dominant than the southeasterly waves (peaks for the northwest signal and nadirs for the southeast signal) when the NAO phase is positive (or less negative), and vice versa when the NAO phase shifts to negative (or less positive). In overall, good correlation is obtained for the open North Atlantic locations ($R^2 = 0.61 - 0.76$), while for the North Sea locations, the correlation on the omnidirectional signal is slightly weaker

$(R^2 = 0.41 - 0.63)$.

A reconstruction of mean wave power is performed for a location at Orkney from $1665 - 2005$, as shown in Figure 3, using a combination of proxy indices from $1665 - 1957$, and climate indices from $1957 - 2005$. A high level of inter-annual and multi-decadal variability is observed. A steep increase is seen during the period from 1960s to 1990s, when the sea surface was reported to be getting rougher (Carter and Draper, 1988; Bacon and Carter, 1991). However, our long timescale analysis seems to suggest that the increase was strongly influenced by the variability of the ocean-atmosphere system driven mostly by the NAO. To assess the feasibility of a wave farm, we include 10 and 20 year moving averages (blue and red lines, respectively). Large multi-decadal trend is noticeable, with the largest variability observed $\sim 25\%$ from again 1960s to 1990s. This considerable variation indicates that the available wave power at this open North Atlantic location is an unreliable resource. However, we observe significantly smaller variation when we include the practical wave power take-off for a three-float wave power machine.
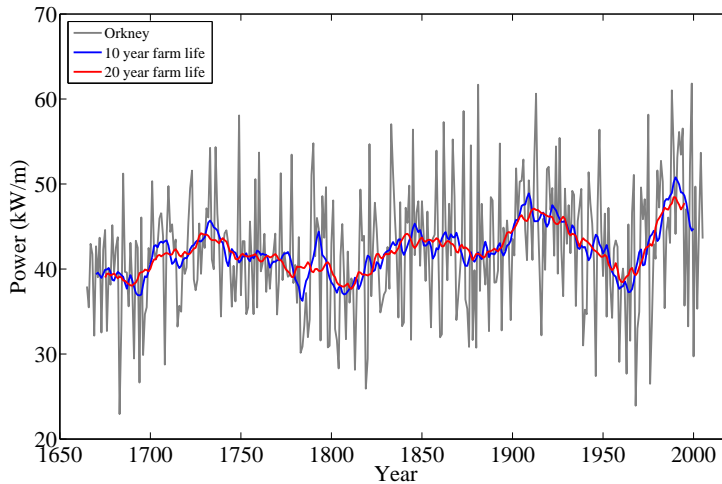

Figure 3: Reconstructed ocean wave power resource for Orkney from $1665 - 2005$. The predictor model uses proxy indices from $1665 - 1957$ and known indices from $1957 - 2005$.

For more details of the analysis on the mean wave power climate variability, see Santo et al. (2015c). The same correlation, angle partitioning and reconstruction method has also been successfully applied to annual mean H_s, T_p, and T_m with comparable R^2 values.

4.1 Practical wave power variability

Having investigated the variability of the ocean wave power resource, we now investigate the variability of wave power produced by a wave energy converter, or the practical wave power, and in this case the M4 machine is chosen. The M4 machine is a three-float system, each float with a circular cross-section when viewed from above and rounded end below the water surface, see Figure 4. Float 1 and float 2 are rigidly connected, and the larger float 3 is connected to float 2 by an articulated joint. The relative angular motion of the joint produces the power take-off. For details of the design principles of the M4 machine, see Stansby et al. (2015b).

The comparison between experiment tests by Stansby et al. (2015a) and numerical modelling by Eatock Taylor et al. (2015) in terms of device performance, or capture width ratio, in irregular waves is satisfactory, see Figure 5. The capture width ratio is defined as the ratio of the average
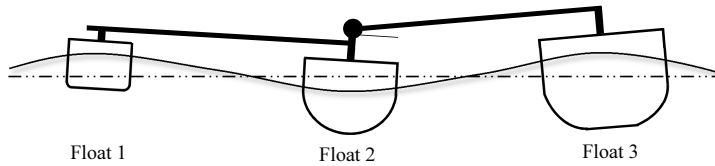
5

Figure 4: Sketch showing motions of the M4 machine during the passage of a wave.

generated power to the ocean wave power resource, normalised by a wavelength. We include this capture width ratio characteristic as well as power clipping to limit power take-off in the practical wave power calculation. We also note that the M4 machine is sized to the long-term mean wave period at each location. Hence one might reasonably expect considerable differences in the temporal structure of the practical wave power as compared to the bare ocean wave power resource.
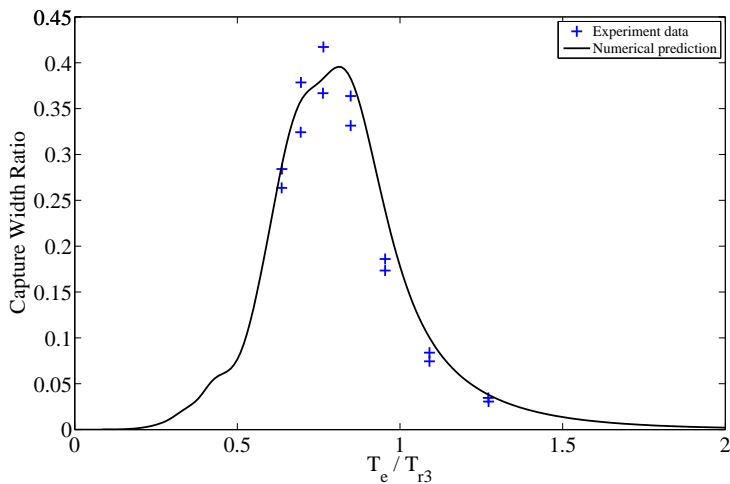

Figure 5: Variation of capture width ratio with ratio of energy period to resonant heave period of stern float (T_e/T_{r3}) for the M4 wave energy converter. Data points are experimental results from Stansby et al. (2015a), solid line is the numerical prediction from Eatock Taylor et al. (2015)

We observe that, after accounting for the power characteristics of the M4 machine and the inclusion of clipping of the power take-off, the temporal variation of the practical wave power across all the locations that we have considered has significantly reduced CV values to $\sim 9\%$, and is still influenced by the climate variability, with R^2 values slightly decreased to $\sim 0.5 - 0.6$, as compared to the variation of the ocean wave power resource. From all the locations considered, Orkney has the highest R^2 value ($R^2 = 0.65$) and also the largest variability (CV = 13%), which brings us to reconstruct the practical wave power at Orkney with the same method as for the ocean wave power previously. The estimated historic practical wave power climate at Orkney from $1665 - 2005$ is shown in Figure 6, with the usual 10 and 20 year moving averages (blue and red lines, respectively). It is apparent that the largest overall variability is now reduced from $\sim 25\%$ (ocean wave power) to $\sim 10\%$ (practical wave power) difference in the power output. This reduction will have consequences for the economic viability of the M4 machine.

Forecasting the power output into the future is difficult as the practical wave climate is still influenced by the natural variability to some extent. However, guided by the reconstruction, we

6

have an idea over the practical range of the power output produced in the past. The most likely production at Orkney, with one M4 machine sized specific to that location, is ~ 315 kW with a long-term possible variation of $\pm 10 - 15\%$ over the assumed life of the farm.
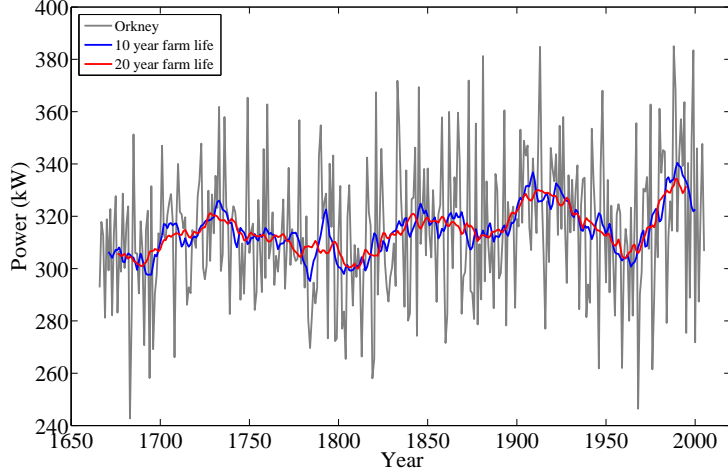

Figure 6: Reconstructed practical wave power resource for Orkney from $1665 - 2005$. The predictor model uses proxy indices from $1665 - 1957$ and known indices from $1957 - 2005$.

For more details of the analysis on the wave power climate variability produced by the M4 machine, see Santo et al. (2015a).

5 Extreme wave climate variability at a 1 in 100 year level

As well as the mean and variation of the mean wave climate, we also investigate extreme wave climate variability using a measure for storm severity, and the correlation with the NAO and other modes. We present results at a 1 in 100 year level. We use the most probable largest individual wave in the storm (H_{mp}) as a representative of storm severity, see Tromans and Vanderschuren (1995). This is a better measure than H_{sMax} within each storm as it accounts for both variation in the H_s and duration of the storm event in a single parameter value. Then extreme value analysis is performed on H_{mp} by using a peaks-over-threshold (POT) technique, and applying the method of maximum likelihood to fit the upper tail of the data with an exponential distribution. To obtain temporal variability of the 1 in 100 year H_{mp}, we apply a five-year sliding window from $1958 - 2011$ with an appropriate threshold value.

From the 3 h H_s and T_p records, we group the record into storms using the same methodology as described in Taylor et al. (2009), and consider only winter storms (from October to March every year). For each storm, we estimate by random sampling (bootstrap) the histogram of H_{max} assuming a Rayleigh distribution of waves within each 3 h interval and JONSWAP spectral shape, and fit the histogram with the empirical probability distribution function (PDF, derived from Rayleigh) by optimising two parameters (σ_s and N_s). These parameters are those of an equivalent storm, with σ_s being the intensity and N_s being the measure of storm duration. The peak value of the empirical PDF (or the mode) is the most probable maximum height of the wave (H_{mp}).

We first investigate the sensitivity of the threshold value used in POT using the entire 54 years of data, and find that 1000 storms is a robust threshold value for all locations. This corresponds
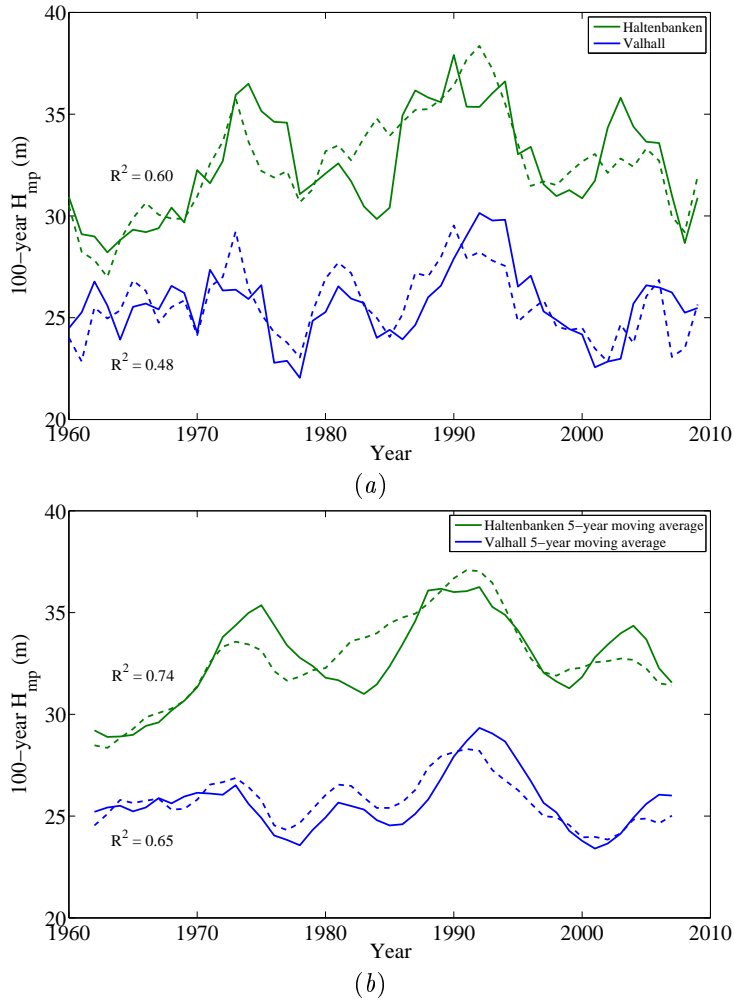
Figure 7: Five-year sliding window results for Haltenbanken (green line) and Valhall (blue line). (a) Comparison in terms of 1 in 100 year H_{mp} (solid lines) and the teleconnection-based prediction (dashed lines). (b) Similar comparison but with an imposed five-year moving average.

to approximately 20 storms per winter, roughly $1 - 2$ per week. We use this threshold value for the extreme value analysis on five-year sliding window basis, and the correlation with the NAO and other modes is analysed on this basis. Figure 7(a) shows the five-year sliding window results of the 1 in 100 year H_{mp} for Haltenbanken and Valhall (solid lines), together with the correlation results (dashed lines). The definition of the storm year is based on the year of December of the third winter, with two winters either side. The long-term variability is apparent from the figure, and it seems to be reasonably correlated with the teleconnections for timescale variation longer than 5 years ($R^2 = 0.50 - 0.60$). This becomes clearer when a five-year moving average is imposed on each signal without doing any further computation, where the correlation is now improved ($R^2 = 0.65 - 0.75$), see Figure 7(b). Hence, we observe that only the long-term variation over 5 years is influenced by the teleconnections, the short-term fluctuation less than 5 years is perhaps dominated by finite size sample variability in the POT analysis.

Good correlation is obtained for locations in the open North Atlantic which are in close proximity to the dominant storm tracks, i.e. Haltenbanken, Schiehallion, Orkney and St Kilda ($R^2 = 0.45 - 0.64$ for five-year sliding window and $R^2 = 0.51 - 0.79$ with imposed five year moving averages). A relationship between the NAO and the extreme wave climate at these locations seems consistent, since the NAO is known to be associated with movements of the storm tracks, and latitude shifts of storm tracks are linked to changes of the largest waves in the North Atlantic, as observed by Lozano and Swail (2002).
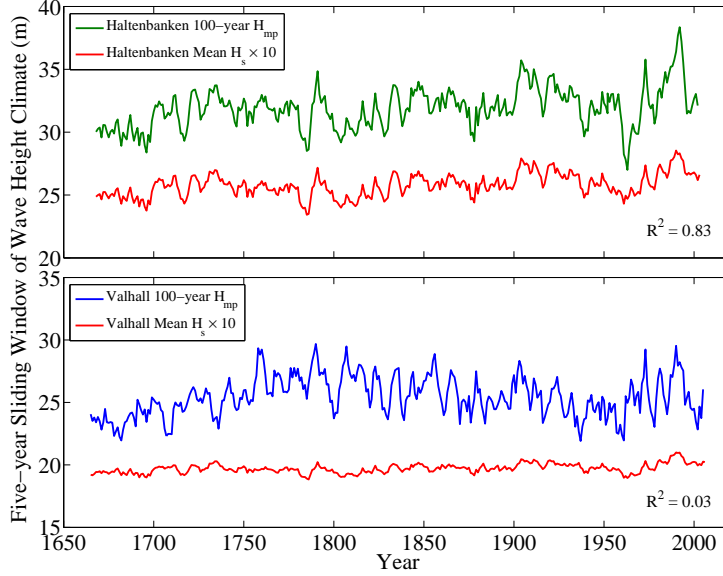

Figure 8: Reconstruction of the extreme (100-year H_{mp}) from $1665 - 2005$ for Haltenbanken (green line) and Valhall (blue line). Also shown is the mean (scaled H_s) wave climate for each location (red lines). The predictor uses proxy indices from 1665 to 1952 and known indices from 1952 to 2005.

With the reasonable correlation with the teleconnections over the period of hindcast data, we perform reconstruction of the 100-year H_{mp} for Haltenbanken and Valhall (green and blue lines, respectively), as shown in Figure 8. Large decadal variation across the record is observed, and there is also an increase in the extreme wave climate during the same period from 1960s to 1990s. The increasing trend is consistent with Vikebø et al. (2003), who performed extreme value analysis on H_{sMax} for locations close to Valhall, Bruce and Haltenbanken.

Also shown in the same figure is the low-pass filtered reconstructed mean annual H_s (5-year moving average, red lines) for both locations. We observe that, in terms of reconstruction, the temporal structures of the extreme and mean wave climates at the open North Atlantic locations close to the dominant storm tracks are very similar ($R^2 = 0.56 - 0.83$), while those at the rest of locations including the North Sea are rather different ($R^2 < 0.20$). The similarity is measured in terms of R^2 as shown in Figure 8 for Haltenbanken and Valhall.

For more details of the analysis on the extreme wave climate variability, see Santo et al. (2015b).

6   Conclusions

In overall, we have investigated the variability of mean and extreme wave climate at locations in the eastern North Atlantic and the North Sea using NORA10 hindcast data. The mean wave climate is assessed in terms of the annual undisturbed ocean resource (kW/m) and also the practical wave power resource extractable using the M4 machine. The inclusion of machine characteristics is essential to assess the economic prospects for any practical wave energy converter. The extreme wave climate is examined in terms of a five-year sliding window of 1 in 100 year of storm severity (H_{mp}), a statistics important for survivability of wave energy converters as well as offshore and marine structures.

In general, we observe that both the extreme and mean wave climates are comparable in the open North Atlantic locations close to the dominant storm tracks: both climates are influenced by the NAO. The wave climates are rather different for the rest of locations including the North Sea: there is more evidence for the mean wave climate to be correlated to the NAO than for the extreme wave climate.

7   Acknowledgement

References

Bacon, S., Carter, D., 1991. Wave climate changes in the North Atlantic and North Sea. International Journal of Climatology 11 (5), 545–558.

Barnston, A. G., Livezey, R. E., 1987. Classification, seasonality and persistence of low-frequency atmospheric circulation patterns. Monthly Weather Review 115 (6), 1083–1126.

Bromirski, P. D., Cayan, D. R., 2015. Wave power variability and trends across the North Atlantic influenced by decadal climate patterns. Journal of Geophysical Research: Oceans.

Carter, D., Draper, L., 1988. Has the north-east Atlantic become rougher? Nature 332, 494.

Eatock Taylor, R., Taylor, P. H., Stansby, P. K., 2015. A coupled hydrodynamic-structural model of the M4 wave energy converter. Journal of Fluids and Structures (under review).

Hurrell, J. W., Kushnir, Y., Ottersen, G., Visbeck, M., 2003. An Overview of the North Atlantic Oscillation. American Geophysical Union.

Izaguirre, C., Mendez, F. J., Menendez, M., Luceño, A., Losada, I. J., 2010. Extreme wave climate variability in southern Europe using satellite data. Journal of Geophysical Research: Oceans (1978–2012) 115 (C4).

Lozano, I., Swail, V., 2002. The link between wave height variability in the North Atlantic and the storm track activity in the last four decades. Atmosphere-Ocean 40 (4), 377–388.

Luterbacher, J., Xoplaki, E., Dietrich, D., Rickli, R., Jacobeit, J., Beck, C., Gyalistras, D., Schmutz, C., Wanner, H., 2002. Reconstruction of sea level pressure fields over the Eastern North Atlantic and Europe back to 1500. Climate Dynamics 18 (7), 545–561.

Mackay, E. B., Bahaj, A. S., Challenor, P. G., 2010. Uncertainty in wave energy resource assessment. Part 2: variability and predictability. Renewable Energy 35 (8), 1809–1819.

Menéndez, M., Méndez, F. J., Losada, I. J., Graham, N. E., 2008. Variability of extreme wave heights in the northeast Pacific Ocean based on buoy measurements. Geophysical Research Letters 35 (22).

Neill, S. P., Hashemi, M. R., 2013. Wave power variability over the northwest European shelf seas. Applied Energy 106, 31–46.

Neill, S. P., Lewis, M. J., Hashemi, M. R., Slater, E., Lawrence, J., Spall, S. A., 2014. Inter-annual and inter-seasonal variability of the Orkney wave power resource. Applied Energy 132, 339–348.

Reguero, B., Losada, I., Méndez, F., 2015. A global wave power resource and its seasonal, interannual and long-term variability. Applied Energy 148, 366–380.

Reistad, M., Breivik, Ø., Haakenstad, H., Aarnes, O. J., Furevik, B. R., Bidlot, J.-R., 2011. A high-resolution hindcast of wind and waves for the North Sea, the Norwegian Sea, and the Barents Sea. Journal of Geophysical Research: Oceans (1978–2012) 116 (C5).

Santo, H., Taylor, P. H., Eatock Taylor, R., Stansby, P. K., 2015a. Decadal variability of wave power production in the North-East Atlantic and North Sea for the M4 machine. Renewable Energy (under review).

Santo, H., Taylor, P. H., Woollings, T., Gibson, R., 2015b. Decadal variability of extreme wave heights as a measure of storm severity in the North-East Atlantic and North Sea. Geophysical Research Letters (under review).

Santo, H., Taylor, P. H., Woollings, T., Poulson, S., 2015c. Decadal wave power variability in the North-East Atlantic and North Sea. Geophysical Research Letters 42 (12), 4956–4963.

Stansby, P., Moreno, E. C., Stallard, T., 2015a. Capture width of the three-float multi-mode multi-resonance broadband wave energy line absorber M4 from laboratory studies with irregular waves of different spectral shape and directional spread. Journal of Ocean Engineering and Marine Energy, 1–12.

Stansby, P., Moreno, E. C., Stallard, T., Maggi, A., 2015b. Three-float broad-band resonant line absorber with surge for wave energy conversion. Renewable Energy 78, 132–140.

Taylor, P., Barker, V., Bishop, D., Eatock Taylor, R., 2009. 100-year waves, teleconnections and wave climate variability. In: 17th International Workshop on Wave Hindcasting and Forecasting, Halifax, Canada.

Tromans, P., Vanderschuren, L., 1995. Response based design method in the north sea: Application of a new method. In: Offshore Technology Conference, OTC 7683, Houston.

Vikebø, F., Furevik, T., Furnes, G., Kvamstø, N. G., Reistad, M., 2003. Wave height variations in the North Sea and on the Norwegian Continental Shelf, 1881–1999. Continental Shelf Research 23 (3), 251–263.

Wang, X. L., Swail, V. R., 2001. Changes of extreme wave heights in Northern Hemisphere oceans and related atmospheric circulation regimes. Journal of Climate 14 (10), 2204–2221.

Woollings, T., Hannachi, A., Hoskins, B., 2010. Variability of the North Atlantic eddy-driven jet stream. Quarterly Journal of the Royal Meteorological Society 136 (649), 856–868.